ORIGINAL ARTICLE
Cell Therapy & Organ Transplantation

JKMS

DOI: 10.3346/jkms.2011.26.4.482 • J Korean Med Sci 2011; 26: 482-491

Establishment of Efficacy and Safety Assessment of Human Adipose Tissue-Derived Mesenchymal Stem Cells (hATMSCs) in a Nude Rat Femoral Segmental Defect Model

Hyung Jun Choi[1,2], Jong Min Kim[2], Euna Kwon[2], Jeong-Hwan Che[2], Jae-Il Lee[2], Seong-Ryul Cho[3], Sung Keun Kang[3], Jeong Chan Ra[3], and Byeong-Cheol Kang[1,2]

[1]Graduate School of Immunology, Seoul National University College of Medicine, Seoul; [2]Department of Experimental Animal Research, Biomedical Research Institute, Seoul National University Hospital, Seoul; [3]Stem Cell Research Center, RNL Bio Co., Ltd., Seoul, Korea

Received: 6 September 2010
Accepted: 17 February 2011

Address for Correspondence:
Byeong-Cheol Kang, PhD
Department of Experimental Animal Research, Biomedical Research Institute, Seoul National University Hospital, 101 Daehak-ro, Jongno-gu, Seoul 110-744, Korea
Tel: +82.2-2072-0841, Fax: +82.2-741-7620
E-mail: bckang@snu.ac.kr

This study was supported by a grant from the Korea Food and Drug Administration.

Human adipose tissue-derived mesenchymal stem cell (hATMSC) have emerged as a potentially powerful tool for bone repair, but an appropriate evaluation system has not been established. The purpose of this study was to establish a preclinical assessment system to evaluate the efficacy and safety of cell therapies in a nude rat bone defect model. Segmental defects (5 mm) were created in the femoral diaphyses and transplanted with cell media (control), hydroxyapatite/tricalcium phosphate scaffolds (HA/TCP, Group I), hATMSCs (Group II), or three cell-loading density of hATMSC-loaded HA/TCP (Group III-V). Healing response was evaluated by serial radiography, micro-computed tomography and histology at 16 weeks. To address safety-concerns, we conducted a GLP-compliant toxicity study. Scanning electron microscopy studies showed that hATMSCs filled the pores/surfaces of scaffolds in a cell-loading density-dependent manner. We detected significant increases in bone formation in the hATMSC-loaded HA/TCP groups compared with other groups. The amount of new bone formation increased with increases in loaded cell number. In a toxicity study, no significant hATMSC-related changes were found in body weights, clinical signs, hematological/biochemical values, organ weights, or histopathological findings. In conclusion, hATMSCs loaded on HA/TCP enhance the repair of bone defects and was found to be safe under our preclinical efficacy/safety hybrid assessment system.

Key Words: Safety; Efficacy; Human Adipose Tissue-Derived Mesenchymal Stem Cells; HA/TCP Scaffold; Bone Defect Model; Nude Rats

INTRODUCTION

The treatment of bone defects remains a challenging problem in orthopedics. Previous studies of bone defect repair rely mainly on the use of fresh autograft bone, bone graft substitutes (1-3), or tissue-engineering techniques that incorporate appropriate implants seeded with cells demonstrating osteogenic potential (3, 4). Human adipose tissue-derived mesenchymal stem cells (hATMSCs) are attractive for tissue-engineering approaches to bone regeneration because they not only demonstrate excellent expansion properties and osteogenic regeneration potential, but also exhibit immunoprivileged or immunomodulatory properties. In addition, scaffolds are required for tissue-engineering applications to deliver cells and act as templates for tissue regeneration. Hydroxyapatite/tricalcium phosphate (HA/TCP) biomaterials can guide bone tissue growth, facilitate bone formation or consolidation, and serve clinically as bone substitutes (5, 6).

Several studies have reported risks associated with the use of mesenchymal stem cells (MSCs). The tumorigenic potential of MSCs was reported in in vitro and in vivo experimental settings using long-term expanded cell populations (7-9). Tasso et al. (10) reported that MSCs induced permanent tumor transformation of adjacent cells when loaded onto bioscaffolds, thus creating tumor niches. For these reasons, preclinical safety testing should be completed prior to the use of MSCs in clinical trials. However, an appropriate system has not been established to evaluate the efficacy and toxicity of MSCs in the context of stem cell properties. Studies of cell transplantation therapies in animal models are often hampered by partial or complete rejection of grafts. To avoid these confounds, we used immunodeficient nude rats as a model for transplantation studies.

In this study, we aimed to establish the preclinical efficacy and safety of a hybrid assessment system for cell-based therapies in a bone defect model using athymic nude rats by 1) determining the capacity of hATMSCs with HA/TCP scaffolds to heal segmental defects, 2) confirming whether hATMSCs exhibit any toxicity in vivo. Our results will contribute to the standardization and implementation of regulatory requirements for new cellular therapies in orthopedics.

pISSN 1011-8934
eISSN 1598-6357

MATERIALS AND METHODS

Isolation and culture of hATMSCs

Adipose tissues were obtained by simple liposuction from the abdominal subcutaneous fat of human donors. All donors provided informed consent, and the donor program was approved by the Institutional Review Board of Seoul National University (IRB No. H-0610-015-186). The subcutaneous adipose tissues were digested with collagenase I (1 mg/mL) under gentle agitation at 37°C for 1 hr. Next, the digested tissues were filtered through a 100 μm nylon sieve to remove cellular debris and centrifuged at 1,500 rpm for 5 min. The pellet was resuspended in DMEM (Invitrogen, Carlsbad, CA, USA)-based media containing 0.2 mM ascorbic acid and 10% fetal bovine serum (FBS). The cell suspension was re-centrifuged at 1,500 rpm for 5 min. The supernatant was discarded and the cell pellet was collected. The cell fraction was cultured overnight at 37°C/5% CO_2 in DMEM-based media containing 0.2 mM ascorbic acid and 10% FBS. Cell adhesion was checked under an inverted microscope the next day. After 24 hr, non-adherent cells were removed and washed with phosphate-buffered saline (PBS). The cell medium was changed to Keratinocyte-SFM (Invitrogen)-based media containing 0.2 mM ascorbic acid, 0.09 mM calcium, 5 ng/mL recombinant epidermal growth factor (rEGF) and 5% FBS. The cells were maintained for four or five days until the cells became confluent, and considered at this point to represent passage 0. When the cells were 90% confluent, they were subculture-expanded in Keratinocyte-SFM-based media containing 0.2 mM ascorbic acid, 0.09 mM calcium, 5 ng/mL rEGF and 5% FBS until passage 3. The immunophenotypes of MSCs were then analyzed using a FACS Calibur Flow Cytometer. Every MSC harvest resulted in a homogenous population of cells with high expression levels of CD73 and CD90 and without expression of CD31, CD34 and CD45. Cell viability evaluated by the trypan blue exclusion method before shipping was > 95%. No evidence of bacterial, fungal, or mycoplasmal contamination was observed in cells tested before shipping. The procedures for MSC preparation were performed under good manufacturing practice (GMP) conditions (RNL BIO, Seoul, Korea).

To assess their MSC character, cells were tested in vitro for mesenchymal multipotency (osteogenic, chondrogenic, adipogenic, neurogenic and myogenic differentiation) before transplantation using lineage-specific stimulation (data not shown).

Preparation of implants and scanning electron microscopy (SEM)

Porous hydroxyapatite/β-tricalcium phosphate (HA/TCP) ceramic blocks (Zimmer, Warsaw, IN, USA), with macropore size of 300-600 μm for and micropore size of ≤ 10 μm, porosity of 60%-70%, and Ca:P ratio of 1.6 were shaped into cylinders approximately 3 mm in diameter and 5 mm in length with a 1 mm wide central canal. The HA/TCP scaffolds were cleaned by sonication, rinsed in distilled water, and then sterilized by gamma radiation. In order to improve their cell-adherent properties, the scaffolds were coated with human fibronectin (100 μg/mL) prior to cell loading. MSC-loaded implants were prepared by incubating human fibronectin-coated HA/TCP scaffolds in a three density of $7.5 \times (10^5$ or 10^6 or $10^7)$ cells/mL suspension of hATMSCs. Two millimeters of cell suspension were added to a 7 mL Vacutainer tube containing the ceramic implants. All loaded carriers were subjected to a vacuum to allow penetration of the MSC suspension. They were then placed in an incubator at 37°C for 3 hr. The loaded carriers were re-fed with cell media overnight and transported to the operating room. Cell-free implants were prepared in a similar fashion by incubating fibronectin-coated scaffolds in a suspension devoid of cells. This procedure was similar to one that was described previously (11).

Cell attachment on the scaffold was confirmed by SEM as previously described (12). Before delivery, specimens of cell-free scaffolds and various densities of cell-loaded scaffolds were fixed in glutaraldehyde (24 hr), dehydrated in ethanol, coated with gold palladium and photographed by SEM.

Animal model and experimental design

All animal experiments were approved by the Institutional Animal Care and Use Committee (IACUC) of the Clinical Research Institute at Seoul National University Hospital (an AAALAC accredited facility), and followed National Research Council (NRC) guidelines for the care and use of laboratory animals (revised 1996). The rat femoral segmental defect model described here is a modification of a previous model used extensively to study long bone repair (11, 13). Twelve-week old adult male athymic nude rats (Harlan, Indianapolis, IN, USA) were used for xenotransplantation experiments. A total of 60 rats were divided into six groups (Table 1). Critical-sized femoral bone defects 5 mm in length were created in the mid-portion of the femoral diaphysis in each rat. In control animals, the bone defects were left empty with cell media. In Group I, the defects were filled with HA/TCP scaffold without any MSCs. In Group II, the defects were filled with hATMSC suspension (cell-loading density: 7.5×10^7 cells/mL) alone to evaluate the therapeutic capacities of MSCs without scaffold. Cell-loaded scaffolds were used to study the effects

Table 1. Experimental design

GROUP	Test item	Cell-loading density
Control	Cell media (empty)	0 cells/mL
I	HA/TCP	0 cells/mL
II	hATMSCs	7.5×10^7 cells/mL
Study group		
III (Low)	hATMSCs + HA/TCP	7.5×10^5 cells/mL
IV (Medium)	hATMSCs + HA/TCP	7.5×10^6 cells/mL
V (High)	hATMSCs + HA/TCP	7.5×10^7 cells/mL

HA/TCP, hydroxyapatite/tricalcium phosphate; hATMSCs, human adipose tissue-derived mesenchymal stem cells.

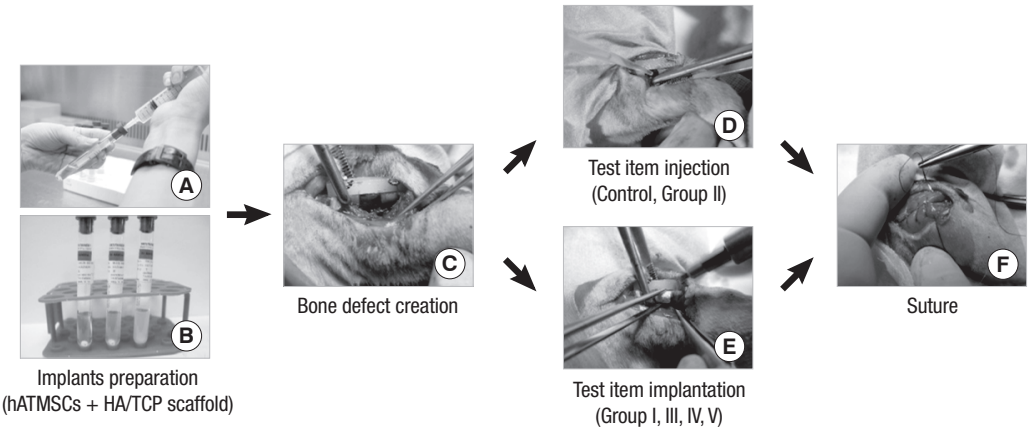

Fig. 1. Procedures for surgical implantation in the femoral segmental defect model from implant preparation to closure. (**A**, **B**) Preparation of the hATMSC-loaded implants, (**C**) femoral segmental defects, (**D**, **E**) transplantation of test items into the defects, (**F**) closure.

of initial cell-loading density on bone tissue formation. Three scaffolds were constructed with cell-loading concentrations of 7.5×10^5 cells/mL (Group III), 7.5×10^6 cells/mL (Group IV), or 7.5×10^7 cells/mL (Group V).

Surgical implantation

Femoral segmental defect surgeries were performed as follows (Fig. 1). Briefly, rats were anesthesized with zoletil/xylazine and prepared aseptically. A longitudinal skin incision was made along the lateral surface of the femoral diaphysis and the overlying periosteum was resected from the defect area. A polyethylene fixation plate (4 × 4 × 23 mm) was secured to the anterolateral aspect of the femur by four 1.1-mm Kirschner wires and two 34G cerclage wires, and a 5 mm transverse segment of the central diaphysis was removed with an oscillating bone saw (Surgic-XT, NSK Nakanishi Inc., Tochigi-ken, Japan) under 0.9% normal saline irrigation. The defect was filled with implants that varied by experimental group (see "Animal model and experimental design", above). Implants were secured by placing two 4-0 Vicryl (Ethicon, Somerville, NJ, USA) sutures around the scaffold and the fixation plate. The muscles were apposed, and the fascia and skin were closed in a routine layered fashion. The animals were allowed full activity in their cages postoperatively.

Efficacy assessment by radiographic analysis

Postoperative radiographs verified implant placement and served as a baseline for radiographic evaluation. Serial radiographs were taken on the day of operation, and at postoperative 4, 8, 12, and 16 weeks, using a high-resolution radiography system (Faxitron 43805N, Hewlett-Packard, McMinnville, OR, USA). The exposure conditions were 40 kV, 1.2 mAs and 6.3 ms. The percentage areas of the femoral segmental defect occupied by newly formed bone were scored as previously described (14). The area percentage of bone regeneration filling the segmental defect and porous materials were graded from 1 to 4 using radiograph. The grades were defined as: [1] < 25% space of -; [2] 25% to 50% space of - ; [3] 50% to 75% space of - ; [4] > 75% space of - segmental defect and/or porous materials filled with new bone. The means of the scores of each group were calculated and compared.

Efficacy assessment by micro-computed tomography (micro-CT) imaging

The representative excised bone specimens were scanned with a Skyscan 1076 (Skyscan, Antwerpen, Belgium) for three-dimensional visualization of new bone formation in the segmental defect. Briefly, the specimens were placed in the holder and the centers of the segmental defects were identified with the scout view window. Femoral defects were scanned using 89 kVp, 112 ms integration time with 0.5 mm filter.

Efficacy assessment by histology and histomorphometry

Sixteen weeks after the surgery, the animals were sacrificed and each defect area was evaluated histologically. The femora were dissected and fixed in 10% neutral-buffered formalin, decalcified (6.5% nitric acid), embedded in paraffin, and cut into 5-μm sections. Specimen histology was examined by hematoxylin and eosin (H&E) staining. Stained sections from each group were observed under a light microscope and were scanned using an attached digital camera and NIS-Elements system (Nikon, Tokyo, Japan). The new bone formation, residual HA/TCP scaffold and connective tissue areas were determined and converted to a percentage of total area of the bone defect with Image Software (Leica Application Suite System, Wetzlar, Germany).

Safety assessment

We conducted a general toxicity study in accordance with good laboratory practices (GLP) and the OECD Guidelines for the Testing of Chemicals (TG409) with some modifications. During the postoperative period, we observed all animals for changes in behavior, general clinical signs, mortality, body weight, and food consumption.

Safety assessment by hematological and biochemical analysis

At 16 weeks after the surgery, hematological analyses were per-

DOI: 10.3346/jkms.2011.26.4.482

formed with an animal blood analyzer (MS 9-5: Melet Schloesing Laboratories, Osny, France), including red blood cell (RBC) count, mean corpuscular volume (MCV), hemoglobin (Hb), mean corpuscular hemoglobin (MCH), mean corpuscular hemoglobin concentration (MCHC), white blood cell (WBC) count, differential WBC count, platelets (PLT), and hematocrit (HCT). Prothrombin time (PT) and activated partial thromboplastin time (APTT) were measured with plasma samples obtained after mixing sodium citrate and centrifuged at 3,000 rpm for 15 min using an automated coagulation analyzer (ACL-100, Lexington, MA, USA). Serum biochemistries were analyzed with an automated chemistry analyzer (Hitachi 7070, Hitachi Co. Ltd., Tokyo, Japan) for the following parameters: total protein (TP), albumin (ALB), A/G, glucose (GLU), cholesterol (CHOL), triglycerides (TG), total bilirubin (TBIL), urea nitrogen (BUN), creatinine (CRE), alanine aminotransferase (ALT), asparate aminotransferase (AST), alkaline phosphatase (ALP), chlorine (Cl), calcium (Ca), potassium (K), and phosphorus (P).

Safety assessment by urinalysis and ocular observations

At sacrifice, we measured the following parameters with a urine analyzer (Miditron Junior II, Roche Diagnostics, Mannheim, Germany): specific gravity, pH, leukocytes, nitrite, protein, glucose, ketones, urobilinogen, bilirubin, and urinary hemoglobin. At the same time points, a veterinarian performed the following ocular examinations: pupillary light reflex (PLR), blink reflex, anterior segment, transparent media, and fundus.

Safety assessment by necropsy, organ weights, and histopathology

At the end of the study the animals were sacrificed by bloodletting under deep anesthesia. Organ weights of the heart, liver, lungs, spleen, kidneys, adrenal glands, testes, brain and pituitary gland were determined by necropsy. Histopathological examinations were performed on the femoral segmental defect (transplantation site), heart, aorta, lungs, trachea, thyroid, parathyroid and salivary glands, stomach, duodenum, jejunum, ileum, colon, adrenals, testes, epididymes, prostate, urinary bladder, skeletal muscles, sciatic nerves, skin, mammary glands, pituitary, eyes, optic nerves, liver, spleen, pancreas, mesenteric lymph nodes, thymus, kidneys, spinal cord and brain. After fixation in 10% neutral-buffered formalin, all tissues were processed in a routine manner, embedded in paraffin, sectioned, and stained with H&E for light microscopic evaluation.

Statistical analysis

Data are presented as means ± SD One-way ANOVA, was performed using SPSS 12.0K to detect and compare differences among groups. For data sets that failed normality or equal variance testing, we used a post hoc Tukey's test or Dunnet's method for subsequent pairwise comparisons. *P* values ($P < 0.05$) indicated significant differences between the control group and treated groups.

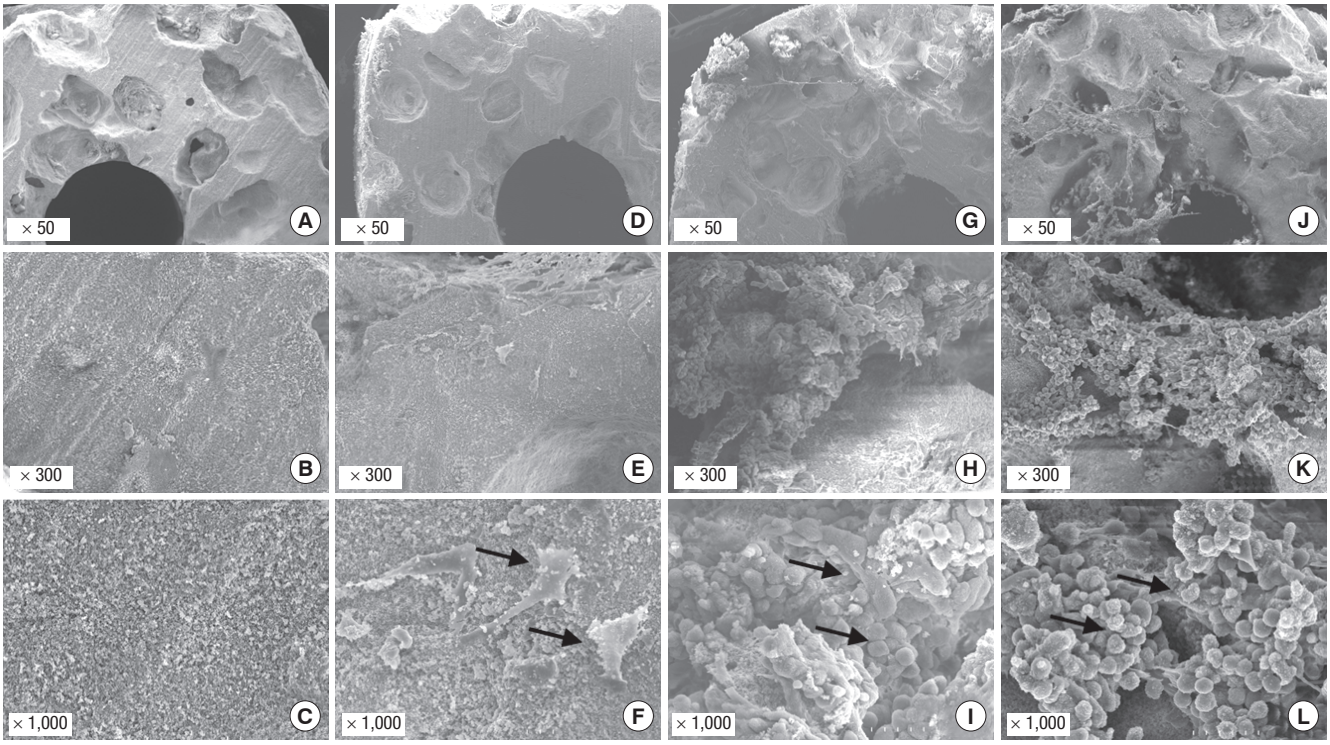

Fig. 2. SEM observations of hATMSC-loaded HA/TCP scaffolds with different cell densities. (**A**-**C**) HA/TCP scaffold, (**D**-**L**) varying density of hATMSC-loaded HA/TCP (**D**-**F**, 7.5 × 10^5 cells/mL; G-I, 7.5 × 10^6 cells/mL; J-L, 7.5 × 10^7 cells/mL). Arrow, attached cells.

RESULTS

Due to two anesthetic deaths, 58 of the original 60 animals were evaluated at follow-up. Among these animals, one nude rat each in Groups I and V showed clinical signs of ataxia and dysplasia of the femur according to serial radiograph (related to pin track infection). The samples from these animals were excluded from the efficacy study.

Efficacy assessed by SEM observations

Cell attachment on scaffolds was confirmed by SEM (Fig. 2). Scanning electron micrographs revealed the ultrastructural architecture of the fibronectin-coated HA/TCP scaffolds. The pores and surfaces of HA/TCP scaffolds were filled with hATMSCs in a cell loading density-dependent manner. In low density cell-loaded scaffolds, the attached cells appeared spindle-like on the scaffold surface. In higher density cell-loaded scaffolds, numerous spherical and spindle cells were detected in the pores and on the surface.

Efficacy assessed by radiographic evaluation

High-resolution Faxitron radiographs provided sufficient clarity and detail to detect subtle changes occurring within the implants and the surrounding host bone (Fig. 3). Defects of control (media) and Group II (hATMSCs alone) rats remained unhealed at 16 weeks. Nonunion at the host bone-implant interfaces occurred in Group I (HA/TCP scaffold alone), and the defect areas appeared granular and fractured. The HA/TCP scaffolds showed incomplete resorption within the 16-week follow-up period. Radiographs demonstrated substantially more bone in animals that received hATMSCs-loaded HA/TCP scaffolds than those that received cell-free HA/TCP scaffolds. Unions between implant and host bone were seen in Groups III, IV and V. The defects in these groups were bridged with radiopaque osteoid tissue that was more radiopaque at higher cell-loading densities. At 12 weeks, union was complete and additional bone was evident in the scaffolds. The scores for percentage areas of the femoral segmental defect occupied by newly formed bone were significantly higher in Group V than in the control group. These differences among the groups were first detected at 4 weeks after implantation and were maintained at 16 weeks after implantation. These data suggest that segmental defects that were filled with hATMSC-loaded HA/TCP scaffolds exhibited new bone formation in a cell loading density-dependent manner.

Efficacy assessed by micro-CT imaging

The defects in each group were visualized by three-dimensional micro-CT imaging (Fig. 4). Defects treated with cell media (control) and hATMSCs alone (Group II) did not close. Defects filled with cell-free HA/TCP scaffolds showed minor bone formation and bridging, but union was not complete. Micro-CT images demonstrate substantially greater bone formation in animals that received hATMSC-loaded HA/TCP scaffolds than in those that received cell-free HA/TCP scaffolds. The newly formed bone was more evenly distributed across the gap in Groups III, IV and V than in controls or Groups I and II.

Efficacy assessed by histological and histomorphometrical evaluation

Photomicrographs of representative sections of the implant groups at 16 weeks are shown in Fig. 5. In controls, most defects were filled with loose fibrous tissue and vessels. Small amounts of callus could be seen in the position on the plate. This pattern was also observed in defects treated with hATMSCs alone in Group II. In defects filled with HA/TCP alone, the tissues around the scaffolds were predominantly filled with fibrous tissue even

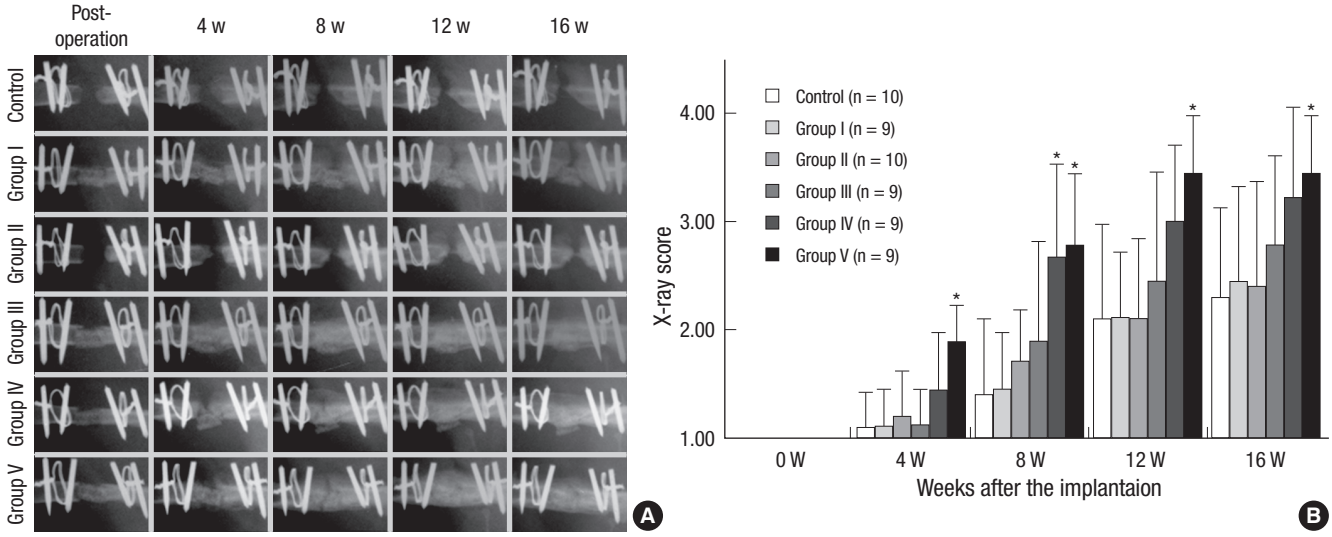

Fig. 3. Radiographs of bone defects treated with hATMSC-loaded HA/TCP scaffolds. (**A**) Serial radiographs at postoperative 0, 4, 8, 12, and 16 weeks. (**B**) The percentage areas occupied by newly formed bone were scored from 1 to 4 (*$P < 0.05$ compared with control).

DOI: 10.3346/jkms.2011.26.4.482

at 16 weeks and most scaffolds remained unabsorbed by 16 weeks. Defects treated with hATMSC-loaded HA/TCP scaffolds in Groups III, IV and V mainly consisted of bone woven into the pores of scaffolds and around the scaffolds. As the amount of loaded cells increased from Groups III to V, more new bone formation was observed and the HA/TCP scaffolds were better absorbed. These signs indicate new bone formation in a cell loading density-dependent manner. These findings were consistent with the results of radiography and micro-CT examinations in these groups. In Group V, the highest density loaded group, large amounts of new bone and marrow were observed in the defects, whereas very little scaffold seemed to be buried in the newly formed osseous tissues. Filling of the pores with new bone and vasculature was evident in regions deeper within the HA/TCP. Despite xenogeneic hATMSC transplantation, no adverse host responses such as lymphocytic infiltration was detected.

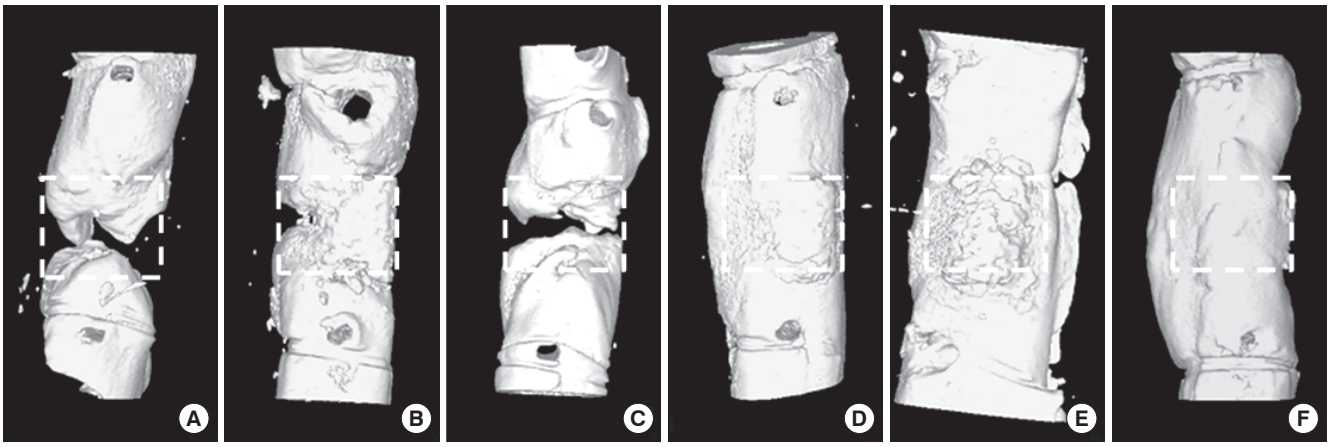

Fig. 4. Micro-computed tomography of bone defects at 16 weeks after surgery. (**A**) Control, (**B**) Group I, (**C**) Group II, (**D**) Group III, (**E**) Group IV, and (**F**) Group V. The dotted box approximately indicates the original defect zone.

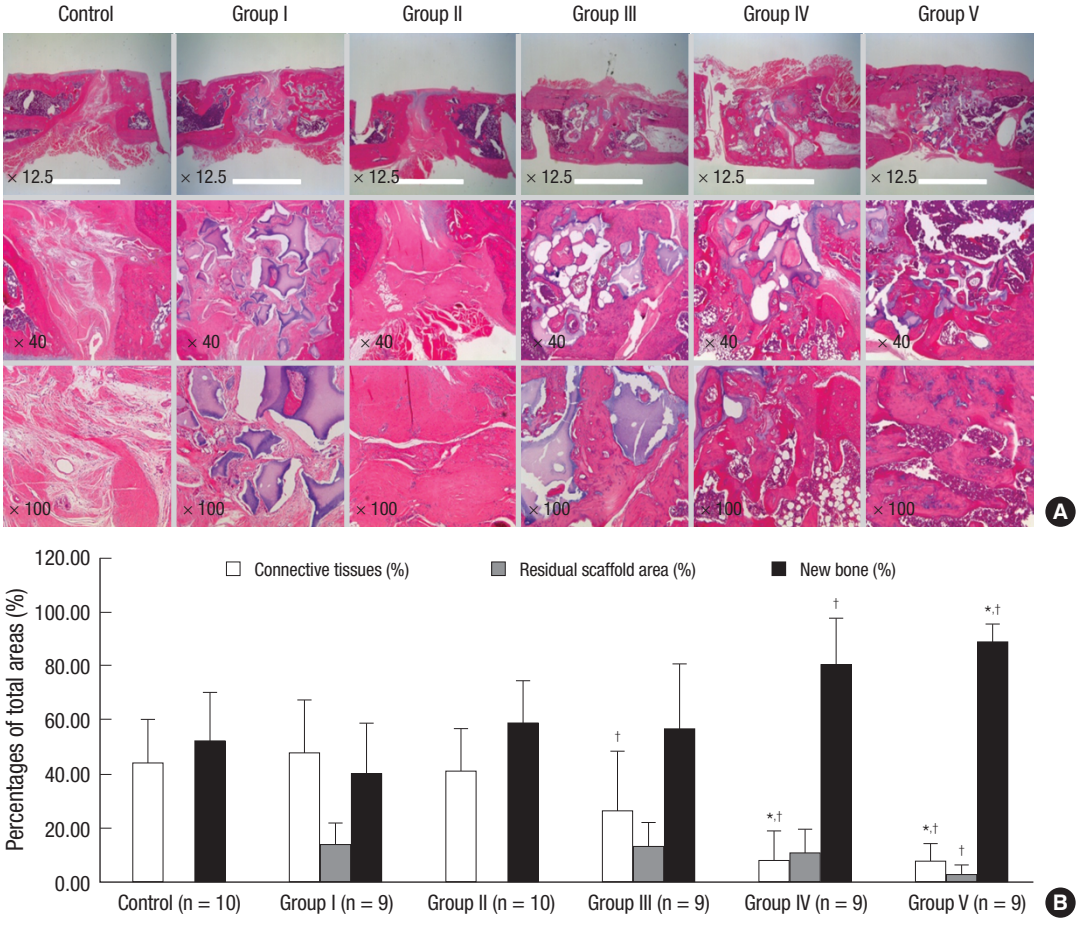

Fig. 5. Histolgical and histomorphometric analysis of bone defects treated with hATMSC-loaded HA/TCP scaffolds at 16 weeks after surgery. (**A**) H&E stain, (**B**) The graphs demonstrate the percentages of connective tissues, residual HA/TCP scaffolds and new bone (*$P < 0.05$ compared with control, †$P < 0.05$ compared with Group I).

Histomorphometric analyses revealed bone in the healed defects of femora treated with low (7.5×10^5 cells/mL), middle (7.5×10^6 cells/mL), and high (7.5×10^7 cells/mL) density hATMSC-HA/TCP scaffolds. The percentages of newly-formed bone were 56.87 ± 23.856 vs 80.72 ± 17.170 vs 89.07 ± 6.518, respectively, indicating patterns of bone formation that increased according to cell-loading density. The bone formation in Groups IV and V was significantly greater than the mean area of bone induced by cell-free HA/TCP scaffolds alone (40.36 ± 18.442), in controls that received only cell media (52.40 ± 17.600), or hATMSCs alone (58.92 ± 15.774). Whereas the residual percentage of HA/TCP scaffolds in Group I was 14.11 ± 7.891, residual percentages of scaffold in Groups III, IV and V were 13.28 ± 8.855, 11.12 ± 8.476, 3.04 ± 3.397, respectively. Percentages of new bone formation and residual scaffold showed an inverse relationship. The percentages of connective tissues in controls and in Group II were 44.15 ± 15.801 and 41.08 ± 15.774, respectively. Whereas the percentage of new connective tissue in Group I was 47.91 ± 19.623, the percentages of new connective tissues in Groups III, IV and V were 26.69 ± 21.620, 8.16 ± 10.746 and 7.89 ± 6.492, respectively.

Safety assessed by mortality, clinical signs, food and water consumption

All follow-up animals survived for the duration of the study. In addition, no adverse clinical signs or symptoms were observed during the experimental period except in the two animals that showed ataxia and dysplasia of femurs mentioned above. There were no significant differences in food and water consumption between control and treated groups (data not shown).

Safety assessed by changes in body weight and hematology

No significant differences in body weights between controls and treated groups were observed during the study period (Fig. 6). No significant differences in hematological parameters were detected (Table 2); hemoglobin, hematocrit, total erythrocyte count, erythrocyte indices (MCV, MCH and MCHC), total leukocyte count, differential leukocyte count, platelet and coagulation time (PT, APTT) were similar across all groups.

Safety assessed by serum biochemistry

Significant increases of BUN and calcium, and significant decreases of phosphorus were observed Group V compared to the control ($P < 0.05$). Significant decreases of chlorine and sodium were observed in Group III compared to the control ($P < 0.05$). However, these differences were considered to be minimal or within normal physiologic limits and not of biologic sig-

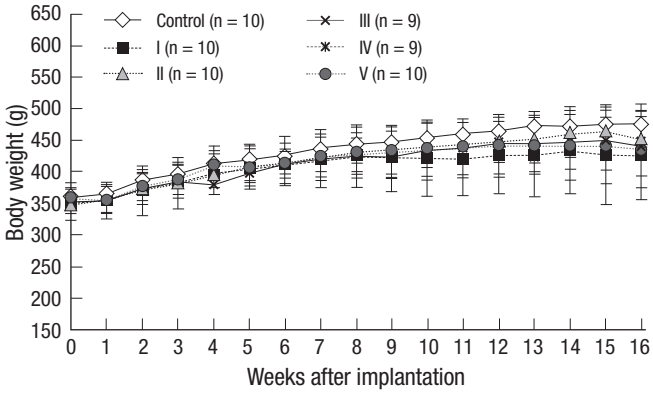

Fig. 6. Body weight changes in nude rats treated with hATMSC-loaded HA/TCP scaffolds. Data are shown as mean ± SD.

Table 2. Hematologic values in nude rats treated with hATMSC-loaded HA/TCP scaffolds

Group items	Control		Group I		Group II		Group III		Group IV		Group V	
	Mean ± SD	No.	Mean ± SD	No.	Mean ± SD	No.	Mean ± SD	No.	Mean ± SD	No.	Mean ± SD	No.
Leukocytes (10^3/μL)	7.51 ± 2.063	10	7.61 ± 3.393	10	7.44 ± 2.650	10	7.04 ± 1.937	9	7.79 ± 3.330	9	7.71 ± 5.976	10
Erythrocytes (10^6/μL)	8.07 ± 0.286	10	7.83 ± 0.841	10	8.17 ± 0.545	10	8.08 ± 0.362	9	7.74 ± 1.076	9	8.06 ± 0.528	10
Hemoglobin (g/dL)	15.0 ± 0.84	10	14.7 ± 1.80	10	15.6 ± 1.11	10	15.4 ± 0.69	9	15.5 ± 1.02	9	15.2 ± 1.19	10
Hematocrit (%)	37.0 ± 1.87	10	36.5 ± 4.72	10	37.4 ± 2.62	10	36.8 ± 1.30	9	36.2 ± 3.42	9	37.6 ± 2.61	10
Platelets (10^3/μL)	1,008 ± 182.2	10	883 ± 311.2	10	994 ± 82.1	10	925 ± 242.5	9	964 ± 259.9	9	984 ± 406.1	10
RBC index												
MCV (fl)	45.8 ± 1.34	10	46.5 ± 1.87	10	45.8 ± 1.40	10	45.6 ± 1.02	9	47.2 ± 3.67	9	46.6 ± 1.41	10
MCH (pg)	18.5 ± 0.66	10	18.8 ± 0.67	10	19.1 ± 0.62	10	19.1 ± 0.33	9	20.4 ± 3.99	9	18.8 ± 0.87	10
MCHC (g/dL)	40.4 ± 1.68	10	40.4 ± 1.87	10	41.6 ± 0.78	10	41.9 ± 0.86	9	42.9 ± 4.40	9	40.4 ± 0.96	10
WBC Differential Counting (%)												
Neutrophils (%)	49.7 ± 9.79	10	53.1 ± 5.40	10	49.6 ± 8.92	10	48.6 ± 9.31	9	47.8 ± 10.08	9	43.8 ± 15.09	10
Eosinophils (%)	0.6 ± 0.28	10	0.7 ± 0.68	10	0.7 ± 0.64	10	0.7 ± 0.61	9	0.7 ± 0.39	9	0.5 ± 0.38	10
Basophils (%)	0.5 ± 0.06	10	0.4 ± 0.13	10	0.6 ± 0.21	10	0.5 ± 0.15	9	0.5 ± 0.21	9	0.5 ± 0.14	10
Lymphocytes (%)	38.5 ± 9.17	10	34.3 ± 5.38	10	38.1 ± 8.01	10	39.9 ± 9.05	9	39.7 ± 8.85	9	44.5 ± 15.17	10
Monocytes (%)	8.8 ± 0.86	10	9.5 ± 1.41	10	9.0 ± 1.17	10	8.5 ± 1.07	9	9.2 ± 1.41	9	8.6 ± 1.98	10
Coagulation												
PT (time)	16.9 ± 1.12	10	15.8 ± 1.62	10	15.8 ± 1.46	10	16.6 ± 1.90	9	16.6 ± 1.63	9	16.2 ± 1.51	10
APTT (time)	23.4 ± 8.81	10	22.4 ± 4.24	10	24.1 ± 4.95	10	26.8 ± 6.73	9	24.6 ± 1.75	9	26.3 ± 2.31	10

SD, standard deviation; RBC, red blood cell; MCV, mean corpuscular volume; MCH, mean corpuscular hemoglobin; MCHC, mean corpuscular hemoglobin concentration; WBC, white blood cell; PT, prothrombin time; APTT, activated partial thromboplastin time.

DOI: 10.3346/jkms.2011.26.4.482

Table 3. Serum biochemical values in nude rats treated with hATMSC-loaded HA/TCP scaffolds

Group items	Control		Group I		Group II		Group III		Group IV		Group V	
	Mean ± SD	No.	Mean ± SD	No.	Mean ± SD	No.	Mean ± SD	No.	Mean ± SD	No.	Mean ± SD	No.
Urea Nitrogen (mg/dL)	17 ± 1.5	10	19 ± 3.9	10	18 ±2.6	10	18 ± 1.5	9	18 ± 1.9	9	22* ± 6.2	10
Cholesterol (mg/dL)	66 ± 14.5	10	60 ± 12.1	10	69 ± 12.9	10	67 ± 10.3	9	68 ± 14.1	9	68 ± 8.0	10
Total Protein (g/dL)	5.2 ± 0.28	10	5.0 ± 0.46	10	5.3 ± 0.33	10	5 ± 0.3	9	5.2 ± 0.27	9	5.1 ± 0.43	10
Albumin (g/dL)	1.9 ± 0.15	10	1.9 ± 0.15	10	2.0 ± 0.17	10	2 ± 0.1	9	1.9 ± 0.13	9	1.9 ± 0.21	10
Total Bilirubin (mg/dL)	0.0 ± 0.03	10	0.0 ± 0.03	10	0.0 ± 0.03	10	0 ± 0.0	9	0.0 ± 0.00	9	0.0 ± 0.00	10
AlkalinePhosphatase (IU/L)	98 ± 22.2	10	140 ± 109.4	10	102 ± 19.1	10	87 ± 11.8	9	105 ± 24.1	9	110 ± 57.8	10
Aspartate Aminotransferase (IU/L)	63 ± 12.1	10	83 ± 62.3	10	66 ± 16.4	10	65 ± 6.1	9	68 ± 15.0	9	82 ± 37.2	10
Alanine Aminotransferase (IU/L)	26 ± 4.0	10	31 ± 6.7	10	28 ± 3.9	10	30 ± 4.0	9	35 ± 12.7	9	33 ± 9.4	10
Creatinine (mg/dL)	0.5 ± 0.05	10	0.6 ± 0.05	10	0.5 ± 0.07	10	1 ± 0.1	9	0.5 ± 0.07	9	0.5 ± 0.10	10
Triglycerides (mg/dL)	26 ± 12.5	10	17 ± 5.6	10	27 ± 10.3	10	25 ± 11.3	9	30 ± 22.2	9	25 ± 11.9	10
Glucose (mg/L)	145 ± 18.5	10	156 ± 74.0	10	142 ± 18.9	10	162 ± 28.3	9	160 ± 29.4	9	151 ± 32.2	10
A/G ratio	1 ± 0.1	10	1 ± 0.1	10	1 ± 0.1	10	1 ± 0.1	9	1 ± 0.1	9	1 ± 0.1	10
Potassium (mM/L)	4 ± 0.3	10	5 ± 0.3	10	5 ± 0.2	10	5 ± 0.2	9	5 ± 0.3	9	5 ± 0.8	10
Chlorine (mM/L)	105 ± 1.4	10	104 ± 3.2	10	105 ± 1.5	10	101* ± 1.8	9	104 ± 1.0	9	103 ± 1.8	10
Calcium (mg/dL)	8.9 ± 0.38	10	8.8 ± 0.45	10	9.0 ± 0.33	10	9 ± 0.3	9	9.2 ± 0.40	9	9.4* ± 0.44	10
Phosphorus (mg/dL)	6 ± 0.6	10	6 ± 0.3	10	6 ± 0.6	10	6 ± 0.5	9	6 ± 0.5	9	7* ± 1.7	10
Sodium (mM/L)	144 ± 1.3	10	144 ± 3.2	10	144 ± 1.8	10	141* ± 2.0	9	143 ± 1.0	9	144 ± 2.7	10

*Significantly different from the control group; $P < 0.05$. SD, standard deviation; hATMSCs, human adipose tissue-derived mesenchymal stem cells; HA/TCP, hydroxyapatite/tricalcium phosphate.

nificance (Table 3).

Safety assessed by ophthalmologic examination and urinalysis

No visible evidence of ocular abnormalities of effects was detected in ophthalmologic examinations. There were no significant differences in the results of urinalysis between control and treated groups (data not shown).

Safety assessed by ophthalmologic organ weights, necropsy findings and histopathological findings

There were no significant differences in the absolute and relative weights of major organs related to detoxification and excretion (liver and kidney), immunity (spleen and thymus), endocrine function (adrenal glands and pituitary gland), circulation (heart), respiration (lung), nervous system (brain) or reproduction (testis) (data not shown) across groups. Results of gross postmortem examinations performed on all animals did not reveal any evidence of visible morphologic abnormalities in any animals used in the study. Histopathologic evaluations showed that the T-cell-dependent regions of thymus, spleen and lymph nodes were reduced or absent of, that were of the lesions seen in the athymic nude rats. There were no indications of any microscopic abnormalities related to the implantations of hATMSCs and HA/TCP scaffolds (data not shown).

DISCUSSION

The efficacy and safety of stem cell therapies must be established in appropriate animal models before clinical application in humans. These models should take into account properties inherent in the stem cell population as well as the expressions of these properties over time. When we evaluate the efficacy and safety of human cells in laboratory animals, we should consider the immune reactions between human cells and host animals. Whereas in autografts and allografts human patients receive human cells in clinical studies of cell therapies, in preclinical studies of cell therapies laboratory animals typically receive human cells, or xenografts. Therefore, immune deficient animals have been widely used in stem cell research for several years (15, 16).

An appropriate testing system has not yet been established for the development of cell therapy for bone repair. We therefore conducted the present hybrid study of the efficacy and general toxicity of hATMSCs and HA/TCP scaffolds in an athymic nude rat bone defect models. We expect that the present study will support the establishment of a preclinical assessment system for MSCs as cell therapies by confirming the toxicity and regeneration of bone in an animal model.

Testing for general toxicity using appropriate models can help to define risks of adverse events and to design clinical monitoring protocols with clear endpoints. The tumorigenic potential of MSCs presents a critical preclinical safety parameter. The same potential for self-renewal that makes stem cell therapy plausible may also promote cancer (17). Tasso et al. (10) observed sarcomas in mice implanted with MSCs/bioscaffolds that originated from the recipient's tissues, which are widely used in tissue engineering approaches. Although many authors describe MSCs as immunologically privileged (18, 19), it is critical to confirm

that MSCs do not elicit immune responses in animal models. To evaluate the potential for immunological rejection and toxicity in the present study, we performed regular blood analyses; and for the same reason, our histological analyses centered on signs of immunological rejection. The methods used in this study may serve to guide the safety assessment of new cell therapies for orthopedics. We recommend the OECD Guidelines for Testing of Chemicals (TG409) for safety assessment of cell therapy, with some modifications. These protocols include 1) behavioral observations, general clinical signs, mortality, body weight and food consumption (the most general indicators of animal health status); 2) hematological and biochemical analysis; 3) urinalysis; 4) ocular observations; 5) necropsy (organ weights, gross examination, histopathological examination); and 6) tumorigenicity (immunodeficient athymic nude rats).

The results of the present safety study indicate that transplantation of hATMSCs with HA/TCP scaffolds into femoral segmental defects is safe without any detectable side effects, or local or systemic rejection. We found no evidence for ectopic tissue formation in histopathological analysis. In an unpublished previous study of tumorigenicity in immunodeficient mouse strains, we observed that hATMSCs also do not form tumors in nude mice.

Concerns regarding bioscaffolds, which serve to retain cells at implant sites, include biocompatibility and susceptibility to degradation without inducing inflammation. In Group II, hATMSCs alone were transplanted into the defect area. These animals showed little bone formation, because cells could not adhere and then were washed out, demonstrating the necessity of scaffolds in this setting. In orthopedics and traumatology a variety of biomaterials have been developed and widely applied in bone defect management and skeletal tissue engineering, with satisfactory clinical outcomes (20). The HA/TCP scaffold that we used in this study consisted of an optimum balance of 60% HA and 40% TCP, because this composition was previously observed to provide optimum performance in terms of controlled resorption and osseous substitution (21, 22). HA and TCP are osteoconductive, porous biomaterials that have similar compositions, structures, and characteristics to native bone with good biocompatibility (5).

We measured bone regeneration both qualitatively and quantitatively using radiographs, micro-CT and histology for efficacy assessment. In this study, HA/TCP alone did not lead to healing of segmental bone defects. Histological and radiographic analyses revealed no fusion in any cases treated with HA/TCP alone, and that the tissues around the scaffolds were predominantly filled with fibrous tissue even at 16 weeks after treatment. A larger amount of residual HA/TCP scaffolds were still visible in Group I than the hATMSCs-loaded scaffolds in Groups III, IV, and V. However, when HA/TCP scaffolds were loaded with hATMSCs, the transplanted cells stimulated more new bone formation as they were resorbed. In terms of cell loading density on HA/TCP, we found that the amounts of new bone formation and the resorption of scaffolds increased with increased cell volumes. This suggests that the new bone formed in a cell loading density-dependent manner, and that greater amounts of loading cells on HA/TCP scaffolds were beneficial for regenerating new bone. These data support the utility of HA/TCP scaffolds as cell-loading carriers in stem cell therapy.

There are several limitations of this study. First, the bone defect model may need to be longer than 5 mm, because callus could be formed spontaneously along the plate. Callus formation was observed along the fixation plate in some samples, as was an occasional eccentric spicule of bone, usually present along the medial aspect of the femur. Second, further studies should conduct mechanical testing such as torsional stiffness and maximum torque. We did not perform such analyses due to the lack of necessary equipment and the need for samples for toxicity study. Further investigations should test this tissue-engineering method in larger animals, before clinical trials in humans. It may also be useful to implement cell tagging techniques to monitor the journeys of transplanted cells in vivo (23-26).

In conclusion, our data support the safety of hATMSCs and their potential for osteogenesis when used with HA/TCP scaffolds in a bone defect model using athymic nude rats. The scaffold used in the present study, HA/TCP, is identified as a promising candidate for bone tissue engineering with hATMSCs. The preclinical efficacy and safety testing performed in this study provides a framework for standardization and implementation of regulatory requirements for emerging stem cell therapies in orthopedics.

REFERENCES

1. Saito N, Okada T, Horiuchi H, Murakami N, Takahashi J, Nawata M, Ota H, Miyamoto S, Nozaki K, Takaoka K. *Biodegradable poly-D,L-lactic acid-polyethylene glycol block copolymers as a BMP delivery system for inducing bone. J Bone Joint Surg Am 2001; 83-A Suppl 1: S92-8.*
2. Ikeuchi M, Dohi Y, Horiuchi K, Ohgushi H, Noshi T, Yoshikawa T, Yamamoto K, Sugimura M. *Recombinant human bone morphogenetic protein-2 promotes osteogenesis within atelopeptide type I collagen solution by combination with rat cultured marrow cells. J Biomed Mater Res 2002; 60: 61-9.*
3. Boo JS, Yamada Y, Okazaki Y, Hibino Y, Okada K, Hata K, Yoshikawa T, Sugiura Y, Ueda M. *Tissue-engineered bone using mesenchymal stem cells and a biodegradable scaffold. J Craniofac Surg 2002; 13: 231-9.*
4. Dong J, Uemura T, Shirasaki Y, Tateishi T. *Promotion of bone formation using highly pure porous beta-TCP combined with bone marrow-derived osteoprogenitor cells. Biomaterials 2002; 23: 4493-502.*
5. Tancred DC, Carr AJ, McCormack BA. *Development of a new synthetic bone graft. J Mater Sci Mater Med 1998; 9: 819-23.*
6. Walsh WR, Vizesi F, Michael D, Auld J, Langdown A, Oliver R, Yu Y, Irie H, Bruce W. *Beta-TCP bone graft substitutes in a bilateral rabbit tibial defect model. Biomaterials 2008; 29: 266-71.*

 DOI: 10.3346/jkms.2011.26.4.482

7. Tolar J, Nauta AJ, Osborn MJ, Panoskaltsis Mortari A, McElmurry RT, Bell S, Xia L, Zhou N, Riddle M, Schroeder TM, Westendorf JJ, McIvor RS, Hogendoorn PC, Szuhai K, Oseth L, Hirsch B, Yant SR, Kay MA, Peister A, Prockop DJ, Fibbe WE, Blazar BR. *Sarcoma derived from cultured mesenchymal stem cells. Stem Cells 2007; 25: 371-9.*
8. Zhou YF, Bosch-Marce M, Okuyama H, Krishnamachary B, Kimura H, Zhang L, Huso DL, Semenza GL. *Spontaneous transformation of cultured mouse bone marrow-derived stromal cells. Cancer Res 2006; 66: 10849-54.*
9. Aguilar S, Nye E, Chan J, Loebinger M, Spencer-Dene B, Fisk N, Stamp G, Bonnet D, Janes SM. *Murine but not human mesenchymal stem cells generate osteosarcoma-like lesions in the lung. Stem Cells 2007; 25: 1586-94.*
10. Tasso R, Augello A, Carida M, Postiglione F, Tibiletti MG, Bernasconi B, Astigiano S, Fais F, Truini M, Cancedda R, Pennesi G. *Development of sarcomas in mice implanted with mesenchymal stem cells seeded onto bioscaffolds. Carcinogenesis 2009; 30: 150-7.*
11. Bruder SP, Kurth AA, Shea M, Hayes WC, Jaiswal N, Kadiyala S. *Bone regeneration by implantation of purified, culture-expanded human mesenchymal stem cells. J Orthop Res 1998; 16: 155-62.*
12. Muraglia A, Corsi A, Riminucci M, Mastrogiacomo M, Cancedda R, Bianco P, Quarto R. *Formation of a chondro-osseous rudiment in micromass cultures of human bone-marrow stromal cells. J Cell Sci 2003; 116: 2949-55.*
13. Kadiyala S, Jaiswal N, Bruder S. *Culture-expanded, bone marrow-derived mesenchymal stem cells can regenerate a critical-sized segmental bone defect. Tissue Eng 1997; 3: 173-85.*
14. Wan C, He Q, Li G. *Allogenic peripheral blood derived mesenchymal stem cells (MSCs) enhance bone regeneration in rabbit ulna critical-sized bone defect model. J Orthop Res 2006; 24: 610-8.*
15. Xia Z, Ye H, Choong C, Ferguson DJ, Platt N, Cui Z, Triffitt JT. *Macrophagic response to human mesenchymal stem cell and poly (epsilon-caprolactone) implantation in nonobese diabetic/severe combined immunodeficient mice. J Biomed Mater Res A 2004; 71: 538-48.*
16. Jager M, Degistirici O, Knipper A, Fischer J, Sager M, Krauspe R. *Bone healing and migration of cord blood-derived stem cells into a critical size femoral defect after xenotransplantation. J Bone Miner Res 2007; 22: 1224-33.*
17. Lawrenz B, Schiller H, Willbold E, Ruediger M, Muhs A, Esser S. *Highly sensitive biosafety model for stem-cell-derived grafts. Cytotherapy 2004; 6: 212-22.*
18. Bartholomew A, Sturgeon C, Siatskas M, Ferrer K, McIntosh K, Patil S, Hardy W, Devine S, Ucker D, Deans R, Moseley A, Hoffman R. *Mesenchymal stem cells suppress lymphocyte proliferation in vitro and prolong skin graft survival in vivo. Exp Hematol 2002; 30: 42-8.*
19. Le Blanc K, Tammik C, Rosendahl K, Zetterberg E, Ringdén O. *HLA expression and immunologic properties of differentiated and undifferentiated mesenchymal stem cells. Exp Hematol 2003; 31: 890-6.*
20. Kim WS, Kim HK. *Tissue engineered vascularized bone formation using in vivo implanted osteoblast-polyglycolic acid scaffold. J Korean Med Sci 2005; 20: 479-82.*
21. Daculsi G, LeGeros RZ, Nery E, Lynch K, Kerebel B. *Transformation of biphasic calcium phosphate ceramics in vivo: ultrastructural and physicochemical characterization. J Biomed Mater Res 1989; 23: 883-94.*
22. Nery EB, Lynch KL, Hirthe WM, Mueller KH. *Bioceramic implants in surgically produced infrabony defects. J Periodontol 1975; 46: 328-47.*
23. Quintavalla J, Uziel-Fusi S, Yin J, Boehnlein E, Pastor G, Blancuzzi V, Singh HN, Kraus KH, O'Byrne E, Pellas TC. *Fluorescently labeled mesenchymal stem cells (MSCs) maintain multilineage potential and can be detected following implantation into articular cartilage defects. Biomaterials 2002; 23: 109-19.*
24. Tatebe M, Nakamura R, Kagami H, Okada K, Ueda M. *Differentiation of transplanted mesenchymal stem cells in a large osteochondral defect in rabbit. Cytotherapy 2005; 7: 520-30.*
25. Shao X, Goh JC, Hutmacher DW, Lee EH, Zigang G. *Repair of large articular osteochondral defects using hybrid scaffolds and bone marrow-derived mesenchymal stem cells in a rabbit model. Tissue Eng 2006; 12: 1539-51.*
26. Yamazoe K, Mishima H, Torigoe K, Iijima H, Watanabe K, Sakai H, Kudo T. *Effects of atelocollagen gel containing bone marrow-derived stromal cells on repair of osteochondral defect in a dog. J Vet Med Sci 2007; 69: 835-9.*

AUTHOR SUMMARY

Establishment of Efficacy and Safety Assessment of Human Adipose Tissue-Derived Mesenchymal Stem Cells (hATMSCs) in a Nude Rat Femoral Segmental Defect Model

Hyung Jun Choi, Jong Min Kim, Euna Kwon, Jeong-Hwan Che, Jae-Il Lee, Seong-Ryul Cho, Sung Keun Kang, Jeong Chan Ra, and Byeong-Cheol Kang

The purpose of this study was to establish a preclinical assessment system to evaluate the efficacy and safety of cell therapies in a nude rat bone defect model. Segmental defects (5 mm) were created in the femoral diaphyses and transplanted with medium, hydroxyapatite/tricalcium phosphate scaffolds (HA/TCP), hATMSCs, or three cell-loading density of hATMSC-loaded HA/TCP. Healing response was evaluated by serial radiography, micro-computed tomography and histology at 16 weeks. To address safety-concerns, we conducted a GLP-compliant toxicity study. SEM studies showed that hATMSCs filled the pores/surfaces of scaffolds in a cell-loading density-dependent manner. We detected significant increases in bone formation in the hATMSC-loaded HA/TCP groups compared with other groups. The amount of new bone formation increased with increases in loaded cell number. No significant hATMSC-related changes were found in a toxicity study. In conclusion, hATMSCs loaded on HA/TCP enhance the repair of bone.